EasyChair Preprint

№ 3893

Free-Surface Viscous Flow over a Depression

Edward Hinton, Andrew Hogg and Herbert Huppert

July 16, 2020

22nd Australasian Fluid Mechanics Conference AFMC2020
Brisbane, Australia, 6–10 December 2020
DOI: 10.14264/uql.2020.xxYY

Free-surface viscous flow over a depression

Edward M. Hinton[1], **Andrew J. Hogg**[2] **and Herbert E. Huppert**[3]

[1] Bullard Laboratories, Department of Earth Sciences, University of Cambridge, Cambridge CB3 0EZ, UK

[2] School of Mathematics, University of Bristol, Bristol BS8 1UG, UK

[3] Institute of Theoretical Geophysics, King's College, University of Cambridge, Cambridge, CB2 1ST, UK

Abstract

The flow of viscous fluid from a line source on an inclined plane containing a topographic depression is studied using a lubrication model. The steady flow is perturbed by the depression. We focus on the regime in which the flow thickness is small relative to the lengthscale of the depression. For shallow depressions, the flow is only slightly perturbed. However, for deeper depressions a large pond of fluid with a horizontal free-surface is observed. This ponding of fluid is associated with the topography having uphill regions, which in the absence of inertia can only be surmounted by developing a deep fluid layer. The accumulation of fluid in the depression leads to a focusing of the flow, which is observed even far downstream of the depression.

Keywords
viscous flow; lubrication theory; lava flows

Introduction

The interaction between free-surface viscous flows and topography occurs in a variety of industrial and environmental settings. Important examples include coating flows, 3D printing, lava flows and glaciers. For a recent review focusing on flows that are driven by gravity see [1].

The present study is primarily concerned with investigating the effect that topography has on lava flows but there are other applications as well. When uninterrupted, lava can flow into urban areas and cause enormous damage. This has motivated the deployment of barriers to divert the flow and research has investigated optimal design practice [8, 3, 6]. There has also been study aimed at accurately predicting the path that lava will take over topography [4]. The algorithm used tracks the path of steepest descent and then adds in some stochasticity to produce uncertainty estimates for the flow path.

One aspect of lava flows that must be incorporated is the sensitivity of the velocity to the flow thickness. Topographic mounds divert the flow, which also leads to flow thickening. Downstream of the mound, the flow may spread a significant distance in the cross-slope direction due to this thickening [5]. Hence, the flow direction at each point depends on the upstream flow as well as the local topography, whether the amplitude is small or large.

In the present paper we investigate how a free-surface viscous flow, supplied from an upstream line source, interacts with an isolated topographic depression on an inclined plane. In a previous paper, we considered the interaction with a topographic mound [5], which can lead to a dry region where there is no fluid. The study of the interaction with a depression is an important adaptation that leads to some new results, which are relevant to forecasting lava flow paths. The aims of this paper are to determine how the flow is focused by the depression, to quantify the increase in flow thickness within the depression and to understand how this influences the flow behaviour further downstream.

We begin by developing a lubrication model for the flow, which is integrated numerically. Although lava has a complex rheology, we consider a viscous Newtonian fluid and focus on the effect of topography to observe its first-order influence. We study how the flow is slightly perturbed by relatively small depressions. However, perturbation to the upstream thickness is not small if the depression has an uphill region. This motivates studying deeper depressions in which a large pond of fluid, with a horizontal free-surface, accumulates. The accumulation arises from the focusing of fluid into the depression, which fills in order for the flow to surmount the uphill topography. The pond has strong effects further downstream from the depression; the flux and the flow thickness is enhanced directly downstream of the depression. Finally, we conclude with some implications of the results.

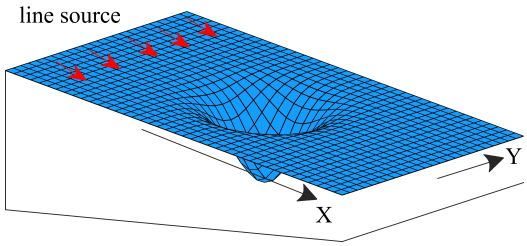

Figure 1. Cartoon of the topography and the upstream line source.

Lubrication model

We analyse a liquid of constant density ρ and viscosity μ released from a line source onto a plane inclined at an angle β to the horizontal. We denotes the downslope coordinate by X, the cross-slope coordinate by Y and the coordinate normal to the plane by Z. We focus on the steady flow that develops and denote the thickness of the current by $H(X,Y)$. The plane contains an isolated topographic depression with shape $Dm(X,Y)$ ($D<0$ and the depression amplitude is $|D|$). The setup is shown in figure 1. Throughout this paper we concentrate on axisymmetric Gaussian depressions with lengthscale L centred on the origin that are described by,

$$m(X,Y)=\exp\left[-(R/L)^2\right], \qquad \text{where} \qquad R^2=X^2+Y^2. \quad (1)$$

We assume that the fluid is sufficiently viscous that both inertial and capillary effects are negligible. We consider depressions that have a lengthscale which is much larger than the flow thickness; $L\gg H$. Thus, we can deploy the sustained line source lubrication approximation to obtain the velocity in the X and Y directions [2, 5]

$$\begin{bmatrix}U\\V\end{bmatrix}=\frac{\rho g}{2\mu}Z(Z-2H)\begin{bmatrix}\left(\frac{\partial H}{\partial X}+D\frac{\partial m}{\partial X}\right)\cos\beta-\sin\beta\\ \left(\frac{\partial H}{\partial Y}+D\frac{\partial m}{\partial Y}\right)\cos\beta\end{bmatrix}, \quad (2)$$

where we have used the conditions of no-slip at the bed ($U = V = 0$ at $Z = 0$) and no stress at the free-surface ($\partial U/\partial Z = \partial V/\partial Z = 0$ at $Z = H$).

The line source supplies a steady flux of Q per unit width. Away from the depression, the flow advances with constant thickness given by [7]

$$H_\infty = \left(\frac{3\mu Q}{\rho g \sin\beta}\right)^{1/3}. \tag{3}$$

We study how this steady flow is perturbed by the depression.

Non-dimensionalisation

We non-dimensionalise the system with the following variables

$$(x,y) = (X,Y)/L, \quad (z,h) = (Z,H)/H_\infty, \quad (u,v) = (U,V)/(Q/H_\infty). \tag{4}$$

The dimensionless flow velocity is

$$\mathbf{u} = 3z(h - z/2)\left[\mathbf{e}_x - \nabla(\mathcal{F}h + \mathcal{M}m)\right], \tag{5}$$

where $\mathbf{e}_x$ is the unit vector in the x direction and

$$\mathcal{F} = \frac{H_\infty}{L\tan\beta}, \qquad \mathcal{M} = \frac{D}{L\tan\beta}. \tag{6}$$

The dimensionless parameter $\mathcal{F}$ quantifies the relative upstream thickness of the flow, whilst $\mathcal{M}$ represents the relative size of the depression; it is the ratio of the characteristic depression gradient, D/L, to the slope gradient, $\tan\beta$. In this paper, we restrict our attention to the case $\mathcal{M} < 0$ corresponding to topographic depressions with $m = \exp(-x^2 - y^2)$. The case of topographic mounds ($\mathcal{M} > 0$) is studied in [5]. The three terms in the square brackets in (5) represent contributions to the velocity associated with the background slope, gradients in the hydrostatic pressure associated with the flow thickness and with the topography, respectively.

The steady governing equation for the flow thickness is obtained by integrating (5) between $z = 0$ and $z = h$ and applying mass continuity [5], to yield

$$\frac{\partial h^3}{\partial x} = \nabla\cdot\left[h^3\nabla(\mathcal{F}h + \mathcal{M}m)\right]. \tag{7}$$

Far from the depression, the steady flow returns to its constant thickness, which imposes the following

$$h \to 1 \quad \text{as} \quad r \to \infty. \tag{8}$$

We focus on the regime $\mathcal{F} \ll 1$ because it is most relevant to the interaction of lava flows with large-scale topography. The regime $\mathcal{F} \ll 1$ and $\mathcal{M} = O(1)$ corresponds to the case in which the current thickness is much less than the depression amplitude and the depression lengthscale.

Numerical results

We solved the steady governing equation numerically using MATLAB's Partial Differential Equation Toolbox™. Full details of the numerical method can be found in [5]. The equation is solved on a rectangular domain with Neumann boundary condition, $h = 1$ on each edge. The size of the numerical domain is increased until further increases lead to less than a 0.1% change in the flow thickness. The figures in this paper show only the most important part of the domain, which includes the depression. Figures 2 and 3 show the steady flow thickness in the cases that $\mathcal{F} = 0.1$ and $\mathcal{M} = -0.8$, and $\mathcal{F} = 0.1$ and $\mathcal{M} = -1.6$, respectively. Note the different scales for the flow thickness. The maximum thickness occurs in the depression on the downstream side. This maximum increases for deeper depressions (more negative $\mathcal{M}$). In the following sections, we seek to understand the flow behaviour through asymptotic analysis.

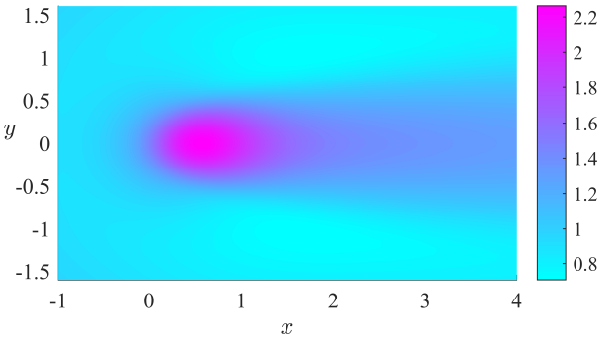

Figure 2. The steady flow thickness, $h(x,y)$, over a depression centred on $(0,0)$. The depression amplitude is $\mathcal{M} = -0.8$ and the flow parameter is $\mathcal{F} = 0.1$.

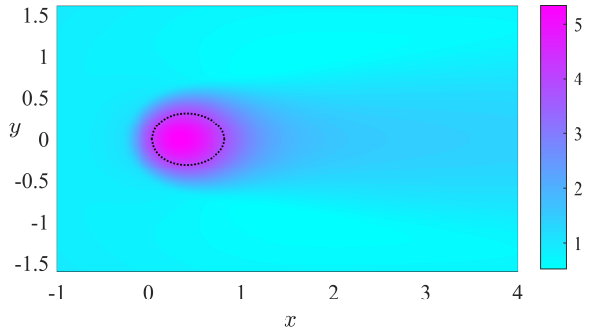

Figure 3. The steady flow thickness, $h(x,y)$, over a depression centred on $(0,0)$. The depression amplitude is $\mathcal{M} = -1.6$ and the flow parameter is $\mathcal{F} = 0.1$. There is a large pond of fluid with a horizontal free-surface in the downstream part of the depression (see figure 8). The boundary of the pond is shown as a dashed line (equation 18).

Small depressions

We begin our analysis for the regime $\mathcal{F} \ll 1$ by following the approach of [5] and seeking a regular expansion for the flow thickness,

$$h = h_0 + \mathcal{F}h_1 + \ldots. \tag{9}$$

Then at leading order the governing equation (7) becomes

$$\left(1 - \mathcal{M}\frac{\partial m}{\partial x}\right)\frac{\partial h_0^3}{\partial x} - \mathcal{M}\frac{\partial m}{\partial y}\frac{\partial h_0^3}{\partial y} = \mathcal{M}h_0^3\nabla^2 m. \tag{10}$$

This first-order equation for h_0 may be studied by the method of characteristics,

$$\frac{\mathrm{d}x}{\mathrm{d}s} = 1 - \mathcal{M}\frac{\partial m}{\partial x}, \quad \frac{\mathrm{d}y}{\mathrm{d}s} = -\mathcal{M}\frac{\partial m}{\partial y}, \quad \frac{\mathrm{d}\log(h_0^3)}{\mathrm{d}s} = \mathcal{M}\nabla^2 m, \tag{11}$$

where s parameterises the characteristics. These equations may be integrated to obtain the leading order solution by applying the boundary condition $h = 1$ far upstream. The characteristic projections in the (x, y) plane are given by

$$\frac{\mathrm{d}y}{\mathrm{d}x} = \frac{-\mathcal{M}\frac{\partial m}{\partial y}}{1 - \mathcal{M}\frac{\partial m}{\partial x}}. \tag{12}$$

Figure 4 shows the characteristic projections in $y \geq 0$ in the case that $\mathcal{M} = -0.8$. For this value of $\mathcal{M}$, the projections access the entire plane and do not intersect since $\mathrm{d}x/\mathrm{d}s > 0$ everywhere. The regular expansion (9) is valid everywhere. Hence the flow thickness, h, is order 1.

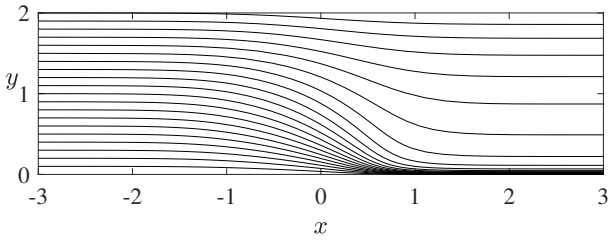

Figure 4. Characteristic projections (equation 12) for h_0 in the case that $\mathcal{M} = -0.8$.

The leading order term, h_0, governed by (11), converges to a fixed shape in y far downstream ($h_0 \approx h_0(y) \neq 1$ for $x \gg 1$). This contrasts with the full solution in which h tends to 1 far downstream. The difference arises because the effect of cross-slope diffusive slumping was neglected in deriving h_0. The diffusive slumping acts to smooth the shape downstream of the mound. Figure 5 shows the difference, $h - h_0$, between the numerical solution and the leading order term for $\mathcal{M} = -0.5$ and $\mathcal{F} = 0.03$. The agreement is good within and upstream of the depression. However, the error associated with the diffusive slumping can be observed downstream. The slumping causes fluid to migrate from the centre, where the thickness increases owing to the depression, outwards.

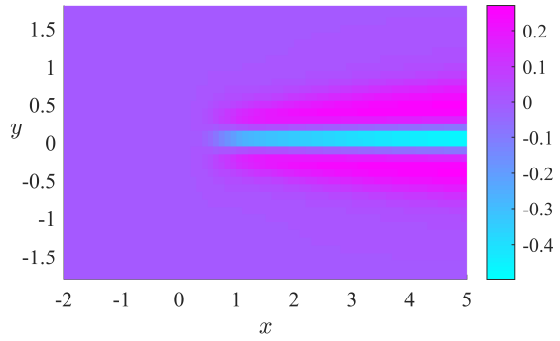

Figure 5. Difference between the numerical solution and the leading order asymptotic solution, $h - h_0$, in the case that $\mathcal{M} = -0.5$ and $\mathcal{F} = 0.03$. The agreement is excellent upstream but deteriorates downstream of the depression.

For deeper depressions, there is a region in which the leading order term h_0 is not defined. Figure 6 shows the characteristic projections in $y \geq 0$ in the case that $\mathcal{M} = -1.6$. In this case, the characteristics can have turning points; there is a region in which $\mathrm{d}x/\mathrm{d}s < 0$. Some of the characteristics converge to a single point and the regular expansion (9) is no longer valid so a different asymptotic expansion is required.

The criteria for the characteristics not to converge to a single point is that

$$\mathrm{d}x/\mathrm{d}s = 1 - \mathcal{M}\frac{\partial m}{\partial x} > 0 \qquad \text{everywhere.} \tag{13}$$

For a Gaussian depression, $m = \exp(-r^2)$, this is equivalent to bounding the amplitude of the depression by

$$0 > \mathcal{M} > \mathcal{M}_c = -(e/2)^{1/2} \approx -1.16\ldots \tag{14}$$

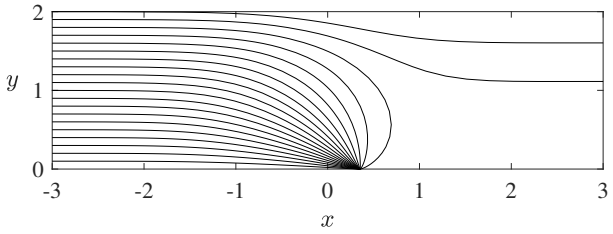

Figure 6. Characteristic projections (equation 12) for h_0 in the case that $\mathcal{M} = -1.6$. Some of the characteristics intersect.

The condition $1 - \mathcal{M}\partial m/\partial x > 0$ is equivalent to the topography being downhill, which is illustrated for the case of $\mathcal{M} = -0.8$ in figure 7. For $\mathcal{M} = -1.6$, there are regions in which the topography is upslope (between the red dots in figure 8). A deep pond develops here, which we study in the next section.

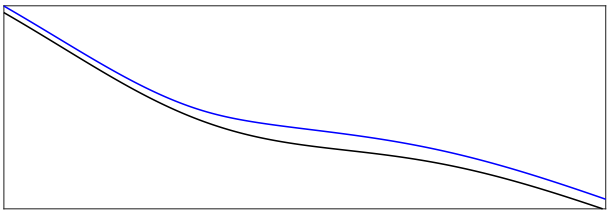

Figure 7. Schematic of the topography (black line) and fluid free-surface (blue line) along the centreline for $\mathcal{M} = -0.8$, $\mathcal{F} = 0.1$. Note that the topography is downhill everywhere.

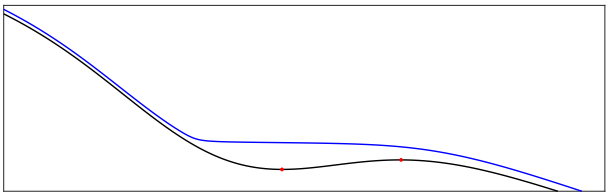

Figure 8. Schematic of the topography (black line) and fluid free-surface (blue line) along the centreline for $\mathcal{M} = -1.6$, $\mathcal{F} = 0.1$. The topography is uphill between the two red dots. A pond with a horizontal free-surface develops within the depression (cf. figure 3).

Deeper depressions

We have shown that in the regime $\mathcal{F} \ll 1$, the flow depth is of order unity when the topography is everywhere downhill. However, when there is an uphill region, a deep pond develops. A pond, with a horizontal free-surface arises because the thin viscous film must deepen to surmount the uphill region (see figure 8). Indeed, a free-surface inclined in the uphill direction would lead to flux in the negative x direction, which is inadmissible.

For $\mathcal{M} < \mathcal{M}_c \approx -1.16$, a pond develops and the flow thickness within, associated with a horizontal free-surface, is given by the following leading order expression

$$h_p = \mathcal{F}^{-1}\left[x - \mathcal{M}m(x,y) + \text{const}\right]. \tag{15}$$

The flow thickness returns to order unity at the downstream edge of uphill region. The most downstream point of this uphill region lies on the centreline and is shown as the right-hand red dot in figure 8. This point is $(x_0, 0)$, where x_0 is the greater root of

$$1 - \mathcal{M}\frac{\partial m}{\partial x} = 0. \tag{16}$$

The pond depth is much less than $\mathcal{F}^{-1}$ at the most downstream point of the uphill region and so we can determine the constant in equation (15),

$$h_p = \mathcal{F}^{-1}\left[x - x_0 - \mathcal{M}(m(x,y) - m(x_0,0))\right]. \qquad (17)$$

The edge of the pond region may then be obtained by setting $h_p = 0$, which yields

$$y^2 = -x^2 - \log\left(\frac{x-x_0}{\mathcal{M}} + e^{-x_0^2}\right). \qquad (18)$$

This curve is plotted as a dotted line in figure 3 and it accurately captures the boundary of the deep region.

The two different regimes described for the flow over a depression are clearly illustrated in figure 9. The maximum flow thickness is plotted as a function of $\mathcal{F}^{-1}$ for $\mathcal{M} = -0.8$ and $\mathcal{M} = -1.6$. For $\mathcal{M} = -0.8$, the maximum flow thickness is insensitive to $\mathcal{F}$. However, with a deeper depression ($\mathcal{M} = -1.6$), the maximum thickness increases linearly with $\mathcal{F}^{-1}$ owing to the pond.

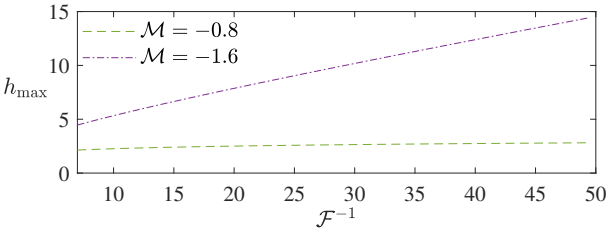

Figure 9. The maximum flow thickness for $\mathcal{M} = -0.8$ and $\mathcal{M} = -1.6$ as a function of $\mathcal{F}^{-1}$.

Downstream effect

We next analyse the effect of the depression on the flow further downstream. The depression focuses the flow from upstream towards the origin. This leads to the development of the deep region within the depression. Downstream of the depression, the flux is greater near the centreline than it is further away because of the upstream focusing. This effect is stronger with deeper depressions. The direction and magnitude of the volume flux is shown as a function of position in figure 10 for $\mathcal{F} = 0.05$ and $\mathcal{M} = -1.6$ (calculated from the numerical solution using equation 5). The flux is significantly enhanced in the centre of the channel downstream of the depression even in regions where the magnitude of the topographic variation, $m(r)$, is very small. The cross-slope slumping terms become significant further downstream and eventually the flow thickness returns to $h = 1$. However, the focusing effect associated with topography, which is observed quite far downstream, is an important consideration when predicting the migration of lava flows.

Conclusions

We have studied the steady interaction between free-surface viscous flows and an isolated topographic depression on an inclined plane. For smaller depressions, the flow thickness is slightly perturbed and this perturbation is smoothed further downstream from the depression. For deeper depressions, large ponds of fluid accumulate. The criteria for this phenomenon is a region in which the topography is uphill. The large pond has strong effects downstream because the flux is concentrated in the shadow of the depression. This focussing is gradually dissipated by cross-slope slumping of the fluid further downstream. A depression can thus substantially alter both the local and the far downstream flow behaviour and this should be considered when forecasting lava flows.

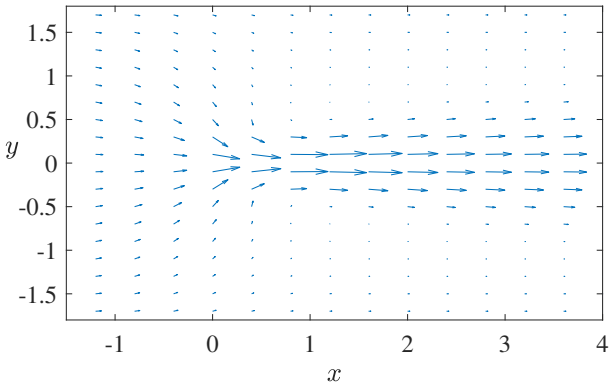

Figure 10. Direction and magnitude of the volume flux for steady flow over a depression for $\mathcal{F} = 0.05$ and $\mathcal{M} = -1.6$.

References

[1] Aksel, N. and Schörner, M. (2018). Films over topography: from creeping flow to linear stability, theory, and experiments, a review. *Acta Mechanica*, 229(4), 1453–1482 (DOI:10.1007/s00707-018-2146-y).

[2] Batchelor, G. K. (1967). An Introduction to Fluid Dynamics. Cambridge university press.

[3] Dietterich, H. R. and Cashman, K. V. and Rust, A. C. and Lev, E. (2015). Diverting lava flows in the lab. *Nature geoscience*, 8(7), 494–496 (DOI:10.1038/ngeo2470).

[4] Favalli, M. and Pareschi, M. T. and Neri, A. and Isola, I. (2005). Forecasting lava flow paths by a stochastic approach. *Geophysical Research Letters*, 32(3) (DOI:10.1029/2004GL021718).

[5] Hinton, E. M. and Hogg, A. J. and Huppert, H. E. (2019). Interaction of viscous free-surface flows with topography. *Journal of Fluid Mechanics*, 876, 912–938 (DOI:10.1017/jfm.2019.588).

[6] Hinton, E. M. and Hogg, A. J. and Huppert, H. E. (2020). Shallow free-surface Stokes flow around a corner. *Philosophical Transactions of the Royal Society A*, 378(2174), 20190515 (DOI:10.1098/rsta.2019.0515).

[7] Lister, J. R. (1992). Viscous flows down an inclined plane from point and line sources. *Journal of Fluid Mechanics*, 242, 631–653 (DOI:10.1017/S0022112092002520)

[8] Scifoni, S. and Coltelli, M. and Marsella, M. and Proietti, C. and Napoleoni, Q. and Vicari, A. and Del Negro, C. (2010). Mitigation of lava flow invasion hazard through optimized barrier configuration aided by numerical simulation: The case of the 2001 Etna eruption. *Journal of Volcanology and Geothermal Research*, 192(1-2), 16–26 (DOI:10.1016/j.jvolgeores.2010.02.002)